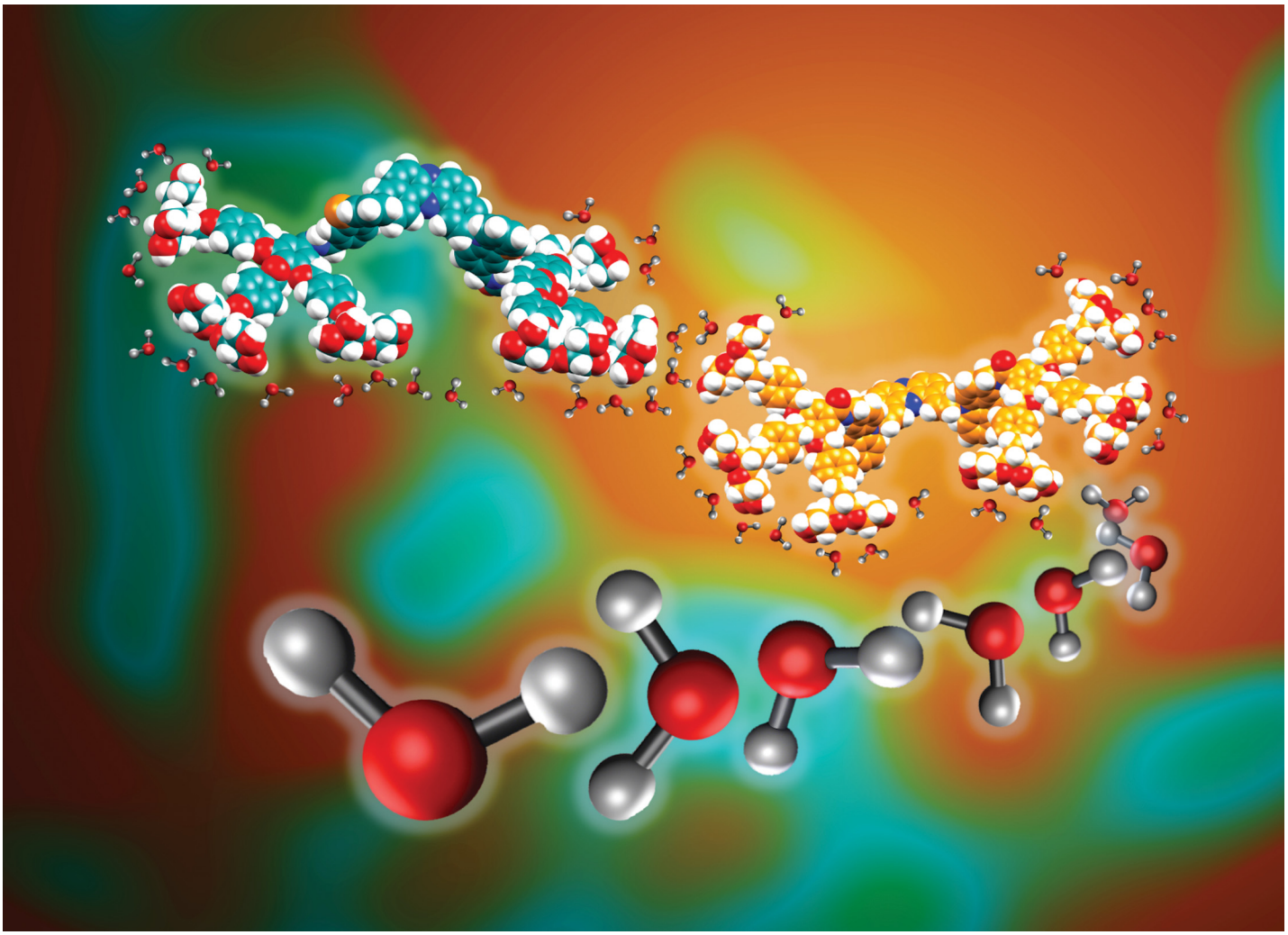

Showcasing research from Professor Takeda's research team, Department of Applied Chemistry, Osaka University, Osaka, Japan.

Water-dispersible donor–acceptor–donor π-conjugated bolaamphiphiles enabling a humidity-responsive luminescence color change

Novel organic donor–acceptor–donor π-conjugated fluorophores that are dispersible in water have been developed. By doping one of the molecules into a hydrophilic polymer, a composite material displaying a humidity-responsive luminescence color change has been fabricated.

As featured in:

See Youhei Takeda *et al.*, *Chem. Commun.*, 2024, **60**, 3653.

ROYAL SOCIETY OF CHEMISTRY

rsc.li/chemcomm

Registered charity number: 207890

ChemComm

COMMUNICATION

View Article Online
View Journal | View Issue

Cite this: *Chem. Commun.*, 2024, **60**, 3653

Received 24th November 2023,
Accepted 6th March 2024

DOI: 10.1039/d3cc05749f

rsc.li/chemcomm

Water-dispersible donor–acceptor–donor π-conjugated bolaamphiphiles enabling a humidity-responsive luminescence color change†

Tomoya Enjou,[a] Shimpei Goto,[a] Qiming Liu,[b] Fumitaka Ishiwari,[acde] Akinori Saeki,[ae] Taro Uemtasu,[a] Yuka Ikemoto,[f] Sora Watanabe,[g] Go Matsuba,[g] Kouichiro Ishibashi,[h] Go Watanabe,[hij] Satoshi Minakata,[a] Yoshimitsu Sagara[bk] and Youhei Takeda*[a]

Novel water-dispersible donor–acceptor–donor π-conjugated bolaamphiphiles, having dibenzophenazine as the acceptor and heteroatom-bridged amphiphilic diarylamines as the donors, have been developed. The materials displayed a distinct photoluminescence color change in response to humidity in a poly(vinylalcohol) matrix.

Organic hydrophobic π-conjugated compounds have found promising applications in the optoelectronics field, such as organic field-effect transistors (OFETs),[1] organic light-emitting diodes (OLEDs),[2] organic lasers (OLs),[3] organic light-emitting transistors (OLETs),[4] and organic photovoltaics (OPVs),[5] due to their electro- and/or photo-active functions arising from the delocalized π-electrons over the entire molecule. However, their use has been severely limited in a non-aqueous environment, due to their intrinsic hydrophobic nature. In contrast, amphiphilic π-conjugated organic molecules, which have a hydrophobic π-conjugated core and amphiphilic/hydrophilic chains, have recently emerged as a new class of functional materials.[6] Amphiphilic nature allows self-assembly of molecules in an aqueous environment to form diverse supramolecular morphologies such as micelles, vesicles, fibers, nanotubes, and H-/J-aggregates, *etc.*[7–12] Also, by making full use of the intrinsic photo- and redox-active functions of the core π-conjugated units and dispersibility in water, they can open up new horizons of materials applications in aqueous environments, such as bio-electronics, bio-imaging, photodynamic therapy, and aqueous photo-catalysis, being complementary to hydrophobic organic π-conjugated compounds.

Herein, we disclose the development of novel π-conjugated bolaamphiphiles **1–4** that have an electronic donor–acceptor–donor (D–A–D) architecture (D = phenoxazine: POZ and phenothiazine: PTZ; A = dibenzo[*a*,*j*]phenazine: DBPHZ) at the central core and six amphiphilic triethylene glycol monomethyl ether (TEGME) and branched polyol units at both edges of the donors (Fig. 1). By making use of the dispersibility in water and charge-transfer (CT) excited state, a humidity-responsive photoluminescence (PL) color change in a hydrophilic polymer film was demonstrated.

To design amphiphilic functional molecules, a DBPHZ-cored D–A–D structure (A = DBPHZ, D = POZ and PTZ)[13] has been chosen as the photoluminescent π-conjugated core, as it exhibits distinct PL arising from the CT excited state. Given that the intensity and wavelength of CT emission is highly sensitive toward the polarity of the microenvironment around the material, humidity detection with amphiphilic D–A–D compounds would be feasible.[14] Furthermore, depending on the population of the predominant conformation of the D–A–D compound with the PTZ donor, the ratio of emissions from local excited

[a] *Department of Applied Chemistry, Graduate School of Engineering, Osaka University, Yamadaoka 2-1, Suita, Osaka 565-0871, Japan. E-mail: takeda@chem.eng.osaka-u.ac.jp*
[b] *Department of Materials Science and Engineering, Tokyo Institute of Technology, 2-12-1 Ookayama, Meguro-ku, Tokyo 152-8552, Japan*
[c] *Frontier Research Base for Global Young Researchers, Graduate School of Engineering, Osaka University, Suita 565-0871, Japan*
[d] *PRESTO, Japan Science and Technology Agency (JST), Kawaguchi, Saitama 332-0012, Japan*
[e] *Innovative Catalysis Science Division, Institute for Open and Transdisciplinary Research Initiatives (ICS-OTRI), Osaka University, Yamadaoka 1-1, Suita, Osaka 565-0871, Japan*
[f] *Japan Synchrotron Radiation Research Institute (JASRI) SPring-8, 1-1-1 Koto, Sayo, Hyogo 679-5198, Japan*
[g] *Graduate School of Organic Materials Science, Yamagata University, Yonezawa, Yamagata 992-8510, Japan*
[h] *Department of Physics, School of Science, Kitasato University, 1-15-1 Kitazato, Minami-ku, Sagamihara, Kanagawa 252-0373, Japan*
[i] *Department of Data Science, School of Frontier Engineering, Kitasato University, 1-15-1 Kitazato, Minato-ku, Sagamihara, Kanagawa 252-0373, Japan*
[j] *Kanagawa Institute of Industrial Science and Technology (KISTEC), 705-1 Shimoimaizumi, Ebina, Kanagawa 243-0435, Japan*
[k] *Living Systems Materialogy (LiSM) Research Group, International Research Frontiers Initiative (IRFI), Tokyo Institute of Technology, 4259 Nagatsuda-cho, Midori-ku, Yokohama, Kanagawa 226-8503, Japan*

† Electronic supplementary information (ESI) available: Synthetic details, spectroscopic data of new compounds, analytical data of DLS, ELS, TEM, IR, TGA, USAXS, and SAXS measurements, and MD simulations. See DOI: https://doi.org/10.1039/d3cc05749f

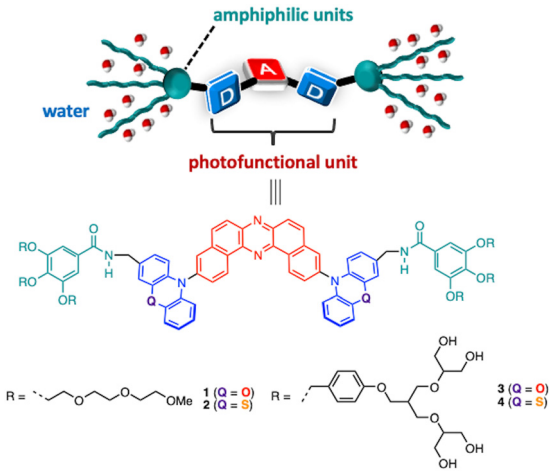

Fig. 1 Chemical structures of bolaamphiphiles **1–4**.

(LE) and CT emission can be tuned.[15] To endow the D–A–D molecules with water-dispersibility, TEGME and dendritic polyol amphiphilic tails were chosen to attach at the edge.[16]

The key synthetic part for **1–4** is illustrated in Scheme S1 (for the details, see the ESI†). With the target compounds in hand, the dispersibility of compounds **1–4** into aqueous media was investigated. Sonication of TEGME-substituted D–A–D compounds **1** and **2** in pure water followed by filtration through a membrane filter (pore size = 50 μm) gave an almost transparent orange and yellowish solution, respectively. But, a slight residue was detected on the membrane filter. To ensure the reproducibility of the dispersion behavior, a small portion of THF solution of **1** and **2** was suspended into water (THF/H_2O, v/v = 5 : 95) followed by filtration through a membrane filter to make a clear aqueous suspension (Fig. S1a and b, ESI†). In contrast, branched polyol-decorated D–A–D compounds **3** and **4** were more easily suspended into pure water without the aid of an organic solvent to provide clear solutions (Fig. S1c and d, ESI†). Dynamic light scattering (DLS) experiments indicated that the hydrodynamic diameter of the self-assembly of **1–4** (mode radius) is 310, 230, 311, and 9.65 & 198 nm, respectively (Fig. S2, ESI†). It is interesting to note that the distribution of particle size for compound **4** has two peaks (Fig. S2d, ESI†). Since the size distribution of **4** was not affected by temperature, there could be an equilibrium between large and small self-assembling particles. The zeta potentials of **1–4** were evaluated by an electrophoretic light scattering (ELS) method to be −28.6, −9.25, −8.94, and −14.1 mV, respectively (Fig. S3, ESI†), suggesting the moderate stability of the nanoparticles in an aquatic environment.[17] Negatively stained transmission electron microscopy (TEM) images revealed the presence of small droplets of a few nm in size (Fig. S4, ESI†). Also, large particles over 100 nm were occasionally found in the samples (Fig. S4c–e, ESI†), which could be responsible for the large mode radius detected by DLS experiments.[18] The smaller particle size observed by TEM than by DLS should arise from the decomposition or shrinkage of the less dense aggregate upon drying on a TEM grid. Ultra small and small angle X-ray scattering (USAXS and SAXS) measurements in aqueous solutions of **1–4** revealed that the D–A–D compounds form large hierarchical assemblies (>100 nm) composed of small aggregates (*i.e.* subunits) with radii of gyration (R_g) ranging from 3.5 to 5 nm (Fig. 3a and Fig. S5, ESI†). The size of the subunits is rationalized by molecular dynamics (MD) simulation (*vide infra*), which is illustrated in Fig. 3b along with the hierarchical assembly structure.

By utilizing the dispersibility in water, UV-Vis absorption spectra of compounds **1–4** in aqueous environments were investigated (Fig. 2). Overall, the spectra of an aqueous solution of **1–4** (solid lines) resembled those in THF (dotted lines), along with a slight red-shift of the spectra (Fig. 2). This observation indicated that D–A–D compounds weakly interact with each other within its self-assembly architecture, although the contribution of solvatochromism is not totally excluded. It should be noted that the absorption spectra of PTZ-bearing compounds **2** and **4** displayed more distinct CT absorption at around 440 nm than their POZ-analogues. This distinct difference is ascribed to the conformational fluctuation of **2** and **4** in the ground state arising from the varied orientation of a substituent on the nitrogen atom of the PTZ donor (*i.e.*, equatorial or axial).[15] Whereas the D–A–D compounds having a POZ donor (*i.e.*, **1** and **3**) adopt almost an orthogonal D–A dihedral angle conformation, the D–A–D compounds having a PTZ donor (*i.e.*, **2** and **4**) adopt an admixture of axial–axial, axial–equatorial, and equatorial–equatorial conformers.[15]

The admixture nature of the conformers for **2** was supported by molecular dynamics (MD) simulation, which was performed for the system in which there are an equal number of molecules of axial–axial and equatorial–equatorial conformers of **2** in water (Fig. 3, Fig. S6, and movie in the ESI†). After the equilibration run, the molecules were spontaneously assembled and formed

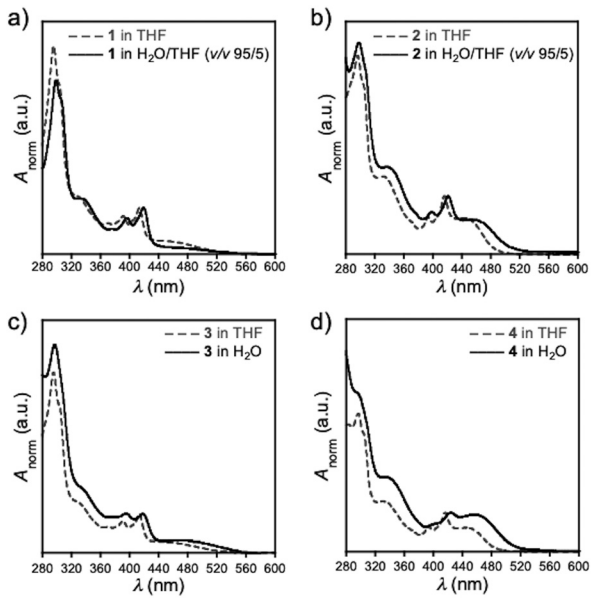

Fig. 2 UV-Vis absorption spectra of (a) **1**, (b) **2**, (c) **3**, and (d) **4** in THF (dotted lines) and an aqueous medium (solid lines).

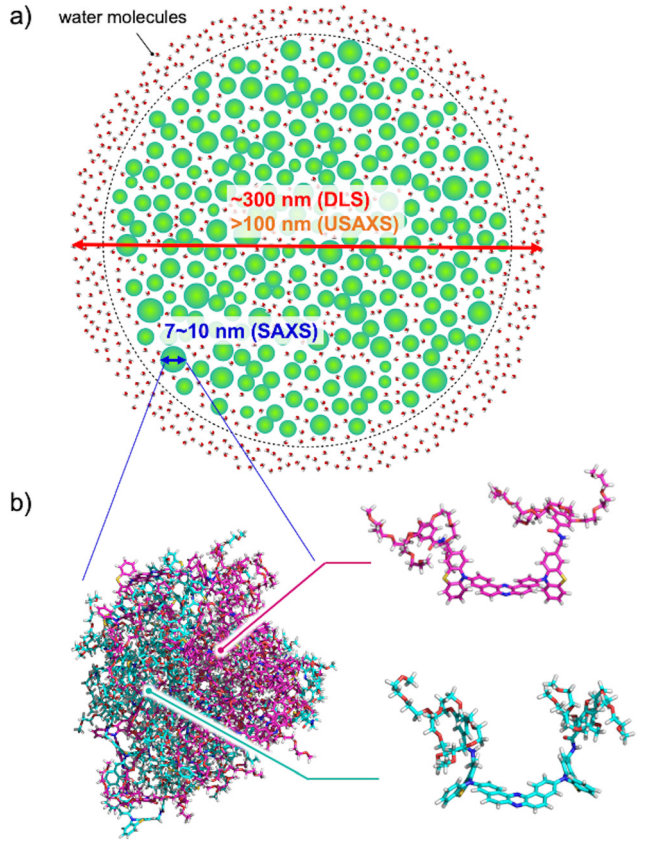

Fig. 3 (a) Hierarchical structure of the aggregate of D–A–D compounds. (b) MD simulation snapshot of the axial–axial and equatorial–equatorial conformers of **2** in water at 200 ns. Axial–axial and equatorial–equatorial conformers are represented by cyan and magenta sticks, respectively. Water molecules are not shown for clarity.

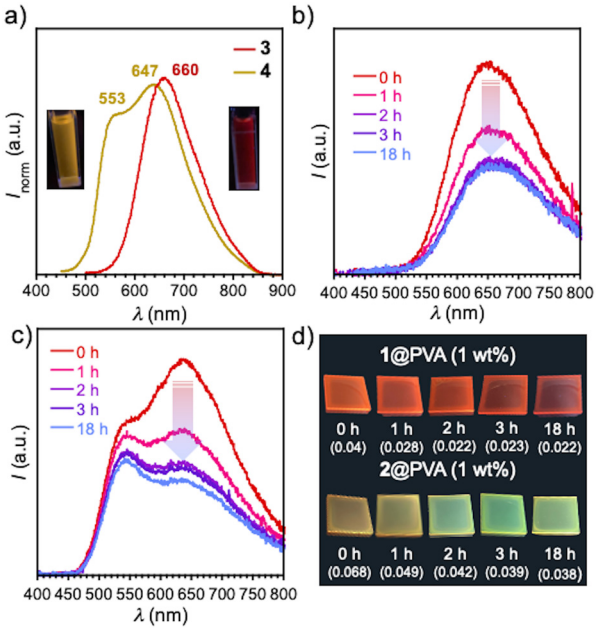

Fig. 4 (a) PL spectra of **3** and **4** in water (c = 10^{-4} M, λ_{ex} = 365 nm) and photographs of **3** and **4** in water taken under the irradiation of UV light (λ_{ex} = 365 nm). (b) PL spectra of **1**@PVA (1 wt%) as a function of time deposited to moisture (RH 75%). (c) PL spectra of **2**@PVA (1 wt%) as a function of time deposited to moisture (RH 75%). (d) Photographs of **1**@PVA and **2**@PVA taken under the irradiation of UV light (λ_{ex} = 365 nm). Values in parentheses indicate PLQY.

nanoscale clusters. Each conformer kept its conformation during the process of assembly. The maximum width of the assembling cluster was approximately 10 nm and its shape was oblate spheroid-like (Fig. 3), in agreement with SAXS experimental results (Fig. S5b; for further discussion on the formation of the hierarchical structure, see the ESI†).

The PL of D–A–D compounds having TEGME chains (**1** and **2**) was quenched in a H_2O-THF medium (PLQY was under the detection limit of 0.01). In contrast, compounds **3** and **4**, which have branched polyol wings at the edge, displayed distinct PL spectra under a relatively high concentration (c = 10^{-4} M), although the PLQY is still under the detection limit (<0.01). The PL are detectable by even the naked eye under UV light (Fig. 4a). It is worth mentioning that PTZ-containing compound **4** displayed a broad dual emission peaked at λ_{em} 553 and 647 nm, while the POZ analogue **3** displayed a Gaussian type PL spectrum peaked at λ_{em} 660 nm (Fig. 4a). The observed dual emission would indicate that different conformers of molecule **4** (ax–ax, ax–eq, and eq–eq) are retained even in the excited state in the self-assembly, which was supported by the different excitation spectra in water (Fig. S7, ESI†). It should be noted that the dual emission of **4** was only observed in water. In polar organic solvents (c = 10^{-4} M in DMSO and DMF), compounds **3** and **4** exhibited emission peaked at around λ_{em} 540, absent in the lower-energy emission (Fig. S8, ESI†). Given that the orientation polarizability (Δf) of water (0.32) is much higher than that of DMSO (0.27) and DMF (0.28), the only lower CT excited state of **4** (excited state for an equatorial-oriented conformer) in polar organic solvents was likely dissipated (Fig. S8, ESI†).

By making full use of the water-dispersible nature of compounds **1** and **2**, homogeneous films (**1**@PVA and **2**@PVA) were fabricated through casting a solution of admixture of water-soluble polymer, poly(vinylalcohol) (PVA), and **1** and **2** (1 wt%) on a quartz plate followed by drying (Fig. 4). Notably, both films **1**@PVA and **2**@PVA displayed distinct PL, which were more visible by the naked eye when compared with PL in solution (Fig. 4b–d). In contrast to **1** and **2**, the PL of compounds **3** and **4** was quenched in the solid state (PLQY < 0.01), probably due to quenching of the excited states by hydroxy groups of the neighboring amphiphilic polyol units through energy transfer to a high-energy vibration level.[19] Thus, only compounds **1** and **2** were applied for the preparation of PVA films. Film **1**@PVA displayed orange-to-red emission with a single peak (λ_{em} = 642 nm, Φ_{PL} 0.04) (Fig. 4b), while film **2**@PVA exhibited yellowish orange emission with double peaks (λ_{em} 533 and 627 nm; Φ_{PL} 0.06). The dual emission from PTZ-containing **2**@PVA should also be ascribed to the presence of different conformers arising from the orientation of the substituent on the nitrogen atom of the donor unit, as suggested by the MD simulation (Fig. 3). Importantly, the PL spectra of the composite films respond to humidity (Fig. 4b–d). After the exposure of **1**@PVA

film to water vapor for 1 h in a bottle filled with NaCl aq. (RH 75%),[20] the emission intensity decreased (Fig. 4b). Intriguingly, in the case of **2**@PVA, only the intensity in the lower-energy emission band was decreased in response to humidity (Fig. 4c). Given that the emission in the lower-energy region is attributed to a CT emission from the equatorial-conformer,[13b,15] the CT emission was partly quenched by water molecules that came into the void of the **2**@PVA film through stabilization of the excited state energy followed by internal conversion, obeying the energy gap law[21] or energy transfer to the vibration level of water.[19] The humidity-responsive PL change for **2**@PVA led to a change in emission color from orange to greenish-yellow (Fig. 4d), while **1**@PVA shows the same emission color. This would allow for visual-sensing of humidity by the naked eye. The time-course profiles of PLQY and PL relative intensity of the composite materials against humidity-exposure time show the exponential decay of the PLQY and relative PL intensity of each emission peak (Fig. S9, ESI†).

To explore the interaction among materials and water molecules, humidity-variable infrared (IR) spectroscopic analysis of D–A–D compound **2** in PVA (1 wt%) and PVA only as a reference was performed (Fig. S10, ESI†). The IR spectra indicated that both films take up water as a function of RH, evident by the increase of absorbance in the O–H stretching band (3000–3800 cm^{-1}). On comparison of the change in absorbance (ΔA) of the two films, the PVA film containing **2** (**2**@PVA) displayed a more significant increase in ΔA than PVA only, indicating the higher hydrophilic character of the film (Fig. S10a, ESI†). The PVA film shows double-peaked absorption at around 3400 cm^{-1} and 3600 cm^{-1} (Fig. S10b, ESI†), which would be ascribed to the O–H stretching bands of isolated water molecules weakly bound to the materials and of small water clusters formed with a few molecules, respectively. In contrast, the film containing D–A–D compound **2** displayed a much broader absorption band over the O–H stretching region (3000–3700 cm^{-1}) (Fig. S10a, ESI†). This would indicate that water molecules existing around the film containing **2** form larger clusters like intermediate water than those in the PVA film.[22] Although the detailed mechanisms await further studies, it is conceivable that the loss of flexibility of water molecules in rotation and motion by forming a hydrogen bonding network through the OH group of PVA, water molecules, and TEGME groups in **2** led to the suppression of non-radiative decay and the manifestation of photoluminescence in the PVA films.

In summary, novel water-dispersible π-conjugated bolaamphiphiles have been developed. The materials form nm-size self-assemblies and display photoluminescence in a water environment. Furthermore, composite films with PVA allow for not only photoluminescence but also visualization of humid environments by the naked eye.

We acknowledge a Grant-in-Aid for Scientific Research on the Innovative Area "Aquatic Functional Materials: Creation of New Materials Science for Environment-Friendly and Active Functions" (JSPS KAKENHI Grant Numbers JP19H05716, JP20H05198, JP22H04531, JP19H05718, JP19H05721, JP19H05717, JP22H04541) and a Grant-in-Aid for Scientific Research (B) (JP23H02037). This work was partially supported by JSPS KAKENHI Grant Number JP23H04878 in a Grant-in-Aid for Transformative Research Areas "Materials Science of Meso-Hierarchy". We acknowledge the Administrative Group of "Aquatic Functional Materials" for supplying D_2O for DOSY experiments (JSPS KAKENHI Grant Number JP19H05714). The synchrotron radiation experiments were performed at the BL19B2 beamline of SPring-8 with the approval of the Japan Synchrotron Radiation Research Institute (JASRI) (Proposal No. 2021A1628, 2022A1797, 2022B0578, and 2022B1963). The computations were partially performed at the Research Center for Computational Science, Okazaki, Japan (Project: 22-IMS-C043 and 23-IMS-C038).

Conflicts of interest

There are no conflicts to declare.

Notes and references

1 C. Wang, H. Dong, W. Hu, Y. Liu and D. Zhu, *Chem. Rev.*, 2012, **112**, 2208.
2 G. Hong, X. Gan, C. Leonhardt, Z. Zhang, J. Seibert, J. M. Musch and S. Bräse, *Adv. Mater.*, 2021, **33**, 2005630.
3 A. J. C. Kuehne and M. C. Gather, *Chem. Rev.*, 2016, **116**, 12823.
4 Z. Qin, H. Gao, H. Dong and W. Hu, *Adv. Mater.*, 2021, **33**, e2007149.
5 G. Zhang, F. R. Lin, F. Qi, T. Heumüller, A. Distler, H.-J. Egelhaaf, N. Li, P. C. Y. Chow, C. J. Brabec, A. K.-Y. Jen and H.-L. Yip, *Chem. Rev.*, 2022, **122**, 14180.
6 L. Zhou, F. Lv, L. Liu and S. Wang, *Acc. Chem. Res.*, 2019, **52**, 3211–3222.
7 (*a*) D. Görl, X. Zhang and F. Würthner, *Angew. Chem., Int. Ed.*, 2012, **51**, 6328; (*b*) Y. Sagara, T. Komatsu, T. Ueno, K. Hanaoka, T. Kato and T. Nagano, *J. Am. Chem. Soc.*, 2014, **136**, 4273.
8 X. Zhang, Z. Chen and F. Würthner, *J. Am. Chem. Soc.*, 2007, **129**, 4886.
9 (*a*) S. H. Seo, J. Y. Chang and G. N. Tew, *Angew. Chem., Int. Ed.*, 2006, **45**, 7526; (*b*) F. J. M. Hoeben, I. O. Shklyarevskiy, M. J. Pouderoijen, H. Engelkamp, A. P. H. J. Schenning, P. C. M. Christianen, J. C. Maan and E. W. Meijer, *Angew. Chem., Int. Ed.*, 2006, **45**, 1232; (*c*) M. R. Molla and S. Ghosh, *Chem. – Eur. J.*, 2012, **18**, 9860; (*d*) T. Xiao, L. Tang, D. Ren, K. Diao, Z.-Y. Li and X.-Q. Sun, *Chem. – Eur. J.*, 2022, e202203463.
10 J.-K. Kim, E. Lee and M. Lee, *Angew. Chem., Int. Ed.*, 2006, **45**, 7195.
11 (*a*) J. P. Hill, W. Jin, A. Kosaka, T. Fukushima, H. Ichihara, T. Shimomura, K. Ito, T. Hashizume, N. Ishii and T. Aida, *Science*, 2004, **304**, 1481; (*b*) E. Lee, J.-K. Kim and M. Lee, *Angew. Chem., Int. Ed.*, 2009, **48**, 3657.
12 H. Maeda, Y. Ito, Y. Haketa, N. Eifuku, E. Lee, M. Lee, T. Hashishin and K. Kaneko, *Chem. – Eur. J.*, 2009, **15**, 3706.
13 (*a*) P. Data, P. Pander, M. Okazaki, Y. Takeda, S. Minakata and A. P. Monkman, *Angew. Chem., Int. Ed.*, 2016, **55**, 5739; (*b*) M. Okazaki, Y. Takeda, P. Data, P. Pander, H. Higginbotham, A. P. Monkman and S. Minakata, *Chem. Sci.*, 2017, **8**, 2677.
14 Y. Cheng, J. Wang, Z. Qiu, X. Zheng, N. L. C. Leung, J. W. Y. Lam and B. Z. Tang, *Adv. Sci.*, 2017, **29**, 1703900.
15 Y. Takeda, H. Mizuno, Y. Okada, M. Okazaki, S. Minakata, T. Penfold and G. Fukuhara, *ChemPhotoChem*, 2019, **3**, 1203.
16 Y. Sagara, T. Komatsu, T. Ueno, K. Hanaoka, T. Kato and T. Nagano, *Adv. Funct. Mater.*, 2013, **23**, 5277.
17 S. Bhattacharjee, *J. Controlled Release*, 2016, **235**, 337.
18 Although the diffusion-ordered NMR spectroscopy (DOSY) experiment of **1** was tried in D_2O, distinct resonance signals were not detected, probably due to the low-solubility in D_2O.
19 J. Maillard, K. Klehs, C. Rumble, E. Vauthey, M. Heilemann and A. Fürstenberg, *Chem. Sci.*, 2021, **12**, 1352.
20 Y. He, J. Guo, X. Yang, B. Guo and H. Shen, *RSC Adv.*, 2021, **11**, 37744.
21 R. Englman and J. Jortner, *Mol. Phys.*, 1970, **18**, 145.
22 M. Tanaka, T. Hayashi and S. Morita, *Polym. J.*, 2013, **45**, 701.

